

# Identification and analysis of alternative splicing events conserved in human and mouse

Gene W. Ye<sup>o\*</sup>†§, Eric Van Nostrand<sup>\*</sup>, Dirk Holste<sup>\*</sup>, Tomaso Poggio<sup>†‡</sup>, and Christopher B. Burge<sup>\*†¶</sup>

Departments of <sup>\*</sup>Biology and <sup>†</sup>Brain and Cognitive Sciences and <sup>‡</sup>Center for Biological and Computational Learning, Massachusetts Institute of Technology, Cambridge, MA 02319

Communicated by Phillip A. Sharp, Massachusetts Institute of Technology, Cambridge, MA, December 30, 2004 (received for review November 23, 2004)

**Alternative pre-mRNA splicing affects a majority of human genes and plays important roles in development and disease. Alternative splicing (AS) events conserved since the divergence of human and mouse are likely of primary biological importance, but relatively few of such events are known. Here we describe sequence features that distinguish exons subject to evolutionarily conserved AS, which we call alternative conserved exons (ACEs), from other orthologous human/mouse exons and integrate these features into an exon classification algorithm, ACESCAN. Genome-wide analysis of annotated orthologous human–mouse exon pairs identified  $\approx 2,000$  predicted ACEs. Alternative splicing was verified in both human and mouse tissues by using an RT-PCR-sequencing protocol for 21 of 30 (70%) predicted ACEs tested, supporting the validity of a majority of ACESCAN predictions. By contrast, AS was observed in mouse tissues for only 2 of 15 (13%) tested exons that had EST or cDNA evidence of AS in human but were not predicted ACEs, and AS was never observed for 11 negative control exons in human or mouse tissues. Predicted ACEs were much more likely to preserve the reading frame and less likely to disrupt protein domains than other AS events and were enriched in genes expressed in the brain and in genes involved in transcriptional regulation, RNA processing, and development. Our results also imply that the vast majority of AS events represented in the human EST database are not conserved in mouse.**

exon skipping | regulatory element | cassette exon | transcriptome | comparative genomics

The processing of human primary transcripts to produce the mRNAs that will direct protein synthesis is often variable, producing multiple alternatively spliced (AS) mRNA products, most commonly by alternative inclusion or exclusion (“skipping”) of individual exons (1–3). Alternative pre-mRNA splicing plays a major role in expanding protein diversity and regulating gene expression in higher eukaryotes (4, 5). Regulated AS is crucial in fruit fly development (3) and in the physiology of the heart, skeletal muscle, brain, and other tissues, and misregulation of AS is associated with human disease (6–8).

EST and cDNA sequence databases provide a rich source of information about splicing events occurring in the human and mouse transcriptomes. Considering the set of human ESTs and cDNAs that can be reliably aligned to a human gene locus overlapping a particular exon, this set can be subdivided into transcripts that include the exon and those that exclude, or skip, the exon in question. Here, the skipping of an exon refers to the situation in which a transcript aligns consecutively to an upstream exon and a downstream exon of a gene, omitting the given exon. This consideration can be applied to all of the exons in a human gene, and an analogous subdivision can be made of the mouse transcripts that align to exons of the orthologous mouse gene. Each orthologous human/mouse exon pair can then be assigned to one of four categories,  $S_{H,M}$ ,  $S_{h,M}$ ,  $S_{H,m}$ , or  $S_{h,m}$ , depending on whether exon skipping has been observed only in human transcripts ( $S_{H,m}$ ), only in mouse ( $S_{h,M}$ ), in both human and mouse ( $S_{H,M}$ ), or not observed in either species ( $S_{h,m}$ ).

By using publicly available EST databases totaling over 5 million human and over 3 million mouse ESTs and databases of  $\approx 94,000$

and  $\approx 91,600$  human and mouse cDNAs, respectively, thousands of alternative exons can be inferred in each species. However, the overlap between these sets is relatively small; i.e., for only  $\approx 240$  ( $\approx 1$  in 18) of the  $\approx 4,500$  conserved human–mouse exons observed to be skipped in human was transcript evidence found supporting alternative usage (skipping) of the orthologous mouse exon, as discussed below (9–11). This observation raises the question of how many of the AS events observable in the human transcriptome are evolutionarily conserved and, therefore, presumably contribute to organismal fitness and how many are aberrant, disease- or allele-specific, or highly lineage-restricted events, which may or may not affect fitness. Although study of the latter types of events may lead to important insights and applications, a significant fraction of these events may constitute biochemical “noise” or transient evolutionary fluctuations. On the other hand, conservation of a specific pattern of AS over the  $\approx 90$  million years since divergence of the mouse and human lineages provides strong evidence of biological function. Therefore, defining the set of AS events conserved between human and mouse is of primary interest in efforts to understand the biological importance of splicing regulation.

Alternative inclusion/exclusion of exons is known to be influenced by a number of factors, such as intron length, exon length, splice site strength and pre-mRNA secondary structure (1, 3, 12). Certain cis-regulatory elements, including exonic splicing enhancers (ESEs), intronic splicing enhancers, exonic splicing silencers (ESSs), and intronic splicing silencers can also control exon skipping by recruiting trans-acting splicing factors (4, 13). Computational studies have identified other sequence features that differ between skipped exons (also known as cassette exons) and constitutive exons in human and mouse genes, including increased conservation in the introns flanking exons skipped in human and mouse (9, 10, 14–16). These observations motivated us to systematically identify, characterize, and integrate sequence features into a classifier that could be used to identify exons subject to evolutionarily conserved exon skipping, here termed alternative conserved exons (ACEs).

## Materials and Methods

**Regularized Least-Squares Classification.** The regularized least-squares classifier was used to learn the features from  $S_{H,M}$  and  $S_{h,m}$  exons and to derive a real-valued output for unlabeled conserved exon pairs. The regularized least-squares classifier has a quadratic loss function and requires the solution of a single system of linear equations,  $(K + \lambda LW^{-1})\mathbf{c} = \mathbf{y}$ , in matrix notation. The goal is to obtain an optimal vector  $\mathbf{c}$ , defined as  $\mathbf{c} = [c_1 \dots c_L]^T$ , where  $L$  is the size of the training set,  $K$  is the  $L \times L$  kernel matrix,  $\lambda$  is the tradeoff between generalization and over-fitting,  $\mathbf{W}$  is the diagonal matrix of

Freely available online through the PNAS open access option.

Abbreviations: AS, alternative splicing; ACE, alternative conserved exon; ESE, exonic splicing enhancer; ESS, exonic splicing silencer; GO, Gene Ontology.

§To whom correspondence may be sent at the present address: Crick–Jacobs Center for Computational and Theoretical Biology, The Salk Institute, La Jolla, CA 92037. E-mail: geneyeo@salk.edu.

¶To whom correspondence may be addressed. E-mail: cburge@mit.edu.

© 2005 by The National Academy of Sciences of the USA

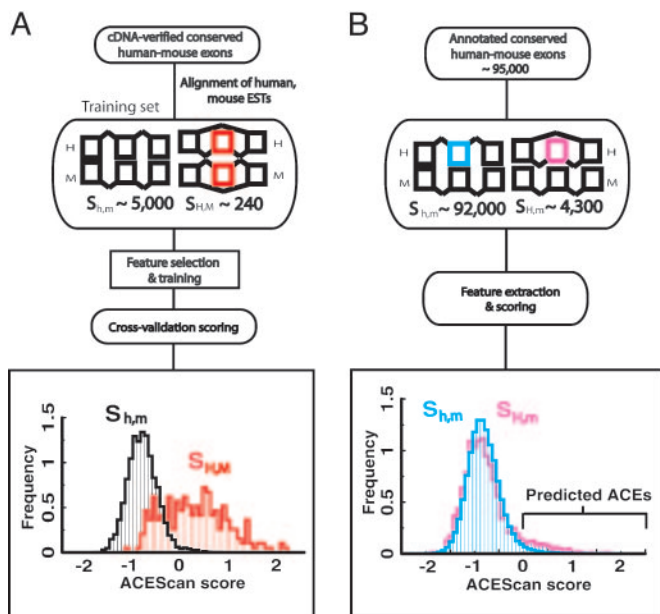


**Fig. 1.** Schematic overview of the learning and prediction stages of the ACESCAN procedure. (A) Learning. Sequence features that differed between sets  $S_{H,M}$  and  $S_{h,m}$  were identified as described (*Supporting Text*). Random subsets of  $S_{H,M}$  and  $S_{h,m}$  were used to train the ACESCAN algorithm, and cross-validation scores were calculated for the unseen subsets of  $S_{H,M}$  and  $S_{h,m}$ . The cross-validated ACESCAN score distributions for  $S_{H,M}$  (red) and  $S_{h,m}$  (black) are shown. (B) Prediction. Spliced alignments of transcript sequences were used to assign ENSEMBL-annotated exons from  $\approx 10,000$  human-mouse orthologous gene pairs (not necessarily alternatively spliced) to one of two sets:  $S_{H,M}$  and  $S_{h,m}$ . ACESCAN score distributions for  $S_{H,M}$  (pink) and  $S_{h,m}$  (blue) are shown.

penalties  $w_i$  (equal to  $\beta$  for positive examples and equal to 1 for negative examples), and  $y$  is the column vector of labels (+1, -1). The algorithm, cross-validation, sampling, and performance measures are described in further detail in *Supporting Text*, which is published as supporting information on the PNAS web site.

**Experimental Validation.** The SuperScript III First-Strand synthesis system for RT-PCR (Invitrogen) was used to generate cDNAs from normal human (fetal brain, fetal liver, cerebellum, heart, whole brain, prostate, liver, lung, kidney, bone marrow, skeletal muscle, and testis) and normal mouse (embryonic mix, whole brain, kidney, skeletal muscle, liver, lung, heart, and testis) tissues by using oligo(dT) primers. The *Taq*DNA polymerase kit (Invitrogen) was used with primers targeted to exons flanking candidate ACEs (further details are given in *Supporting Text*). PCR products of the expected size were gel-purified with the QIAquick Gel Extraction kit (Qiagen, Valencia, CA) and sequenced.

## Results and Discussion

**Outline of Strategy for Identification of ACEs.** Our scheme for identifying ACEs consisted of three phases: learning, prediction, and validation (Fig. 1). In the learning phase, a set of sequence features was identified, including exon and intron length, splice site strength, sequence conservation, and region-specific oligonucleotide composition, which differed between training sets of 241 exons of the class  $S_{H,M}$  and  $\approx 5,000$  exons of the class  $S_{h,m}$  defined above (Fig. 2). For training purposes, exons of the  $S_{h,m}$  class were chosen from genes containing at least one other exon with evidence for AS, because genes lacking AS may experience differing selective pressures than AS genes (17). Next, these features were incorporated into a discriminant classifier, ACESCAN, which was used in the prediction phase to predict which of  $\approx 96,000$  annotated orthologous human/mouse exon pairs not previously known to exhibit

conserved AS are, in fact, ACEs. Finally, in the validation phase, a subset of candidate exons with positive ACESCAN scores (designated ACESCAN[+] exons) was chosen for experimental testing, together with two sets of negative control exons with negative ACESCAN scores (ACESCAN[-] exons): one set with previous transcript evidence for exon skipping in human ( $S_H$  category) and one set lacking such evidence ( $S_h$  category).

The following features were initially incorporated into ACESCAN: (i) exon length, (ii) upstream intron length, (iii) downstream intron length, (iv) 5' splice site score, (v) 3' splice site score, (vi) nucleotide percent identity between orthologous human and mouse exons, (vii) human-mouse intronic sequence conservation within the last 150 bases upstream, and (viii) human-mouse intronic sequence conservation within the first 150 bases downstream of the exon. In general, exon pairs skipped in both human and mouse (set  $S_{H,M}$ ) were observed to be shorter than unskipped exon pairs ( $S_{h,m}$ ), were flanked by longer upstream and downstream introns, and possessed significantly weaker splice sites (Fig. 2). Strikingly, exon pairs in  $S_{H,M}$  have significantly higher sequence identity and higher flanking intronic conservation as compared with exon pairs in  $S_{h,m}$  (Fig. 2). High levels of sequence conservation in the exons and flanking introns is suggestive of conservation of regulatory motifs or RNA structure. These observations are similar to and consistent with previous studies (10, 14–16).

**Oligonucleotides Useful in Discrimination of ACEs.** Oligonucleotide features designed to score potential cis-regulatory elements consisted of the highest-ranking (most biased) overrepresented and underrepresented oligonucleotides of length  $k$  ( $k$ -mers) in different exon and intron regions. The regions considered were the first and last 100 bases of exons and the proximal 150 bases in the upstream and downstream introns flanking the exon, because of the high levels of sequence conservation in these regions and their proximity to the regulated splice junctions. Counts of conserved oligonucleotides in human-mouse nucleotide alignments of the 150 bases of upstream and downstream intronic sequence and in the entire exon were scored for enrichment in the  $S_{H,M}$  set versus the  $S_{h,m}$  set. Inclusion of oligonucleotide counts from aligned and unaligned sequences permits scoring of cis-regulatory elements that do and do not require strict spatial constraints for function.

Oligonucleotides were ranked by their enrichment as measured by a  $\chi^2$  value. Several of the overrepresented intron elements were similar to known intronic regulatory elements (e.g., UGCAUG and UC-rich repeats; Table 1, which is published as supporting information on the PNAS web site, and *Supporting Text*). We propose that a significant fraction of the remaining elements may represent previously uncharacterized intronic regulatory sequences. A number of the overrepresented and underrepresented exon elements (Fig. 2) were similar to ESE hexamers (Table 2, which is published as supporting information on the PNAS web site) identified by using the RESCUE-ESE method or systematic evolution of ligands by exponential enrichment (SELEX) (18, 19) or to ESS elements identified through a recent cell fluorescence-based *in vivo* screen for splicing silencers (20). The relative distribution of these elements suggests that ACEs may have a higher density of ESS sequences than constitutive exons, which would tend to facilitate exclusion by the splicing machinery. The increased frequency of ESS sequences in ACEs relative to constitutive exons might reflect differing selective pressures, with constitutive exons presumably being under selection for efficient exon inclusion, whereas alternative exons are presumably selected for inefficient inclusion under at least some conditions (e.g., in specific cell types or developmental stages).

**Integration and Selection of Features for Accurate Exon Classification.** The task of integrating the general features and oligonucleotide features described above into an algorithm that distinguishes exon pairs in  $S_{H,M}$  (positively labeled) from those in  $S_{h,m}$  (negatively labeled) was posed as a supervised binary classification problem.

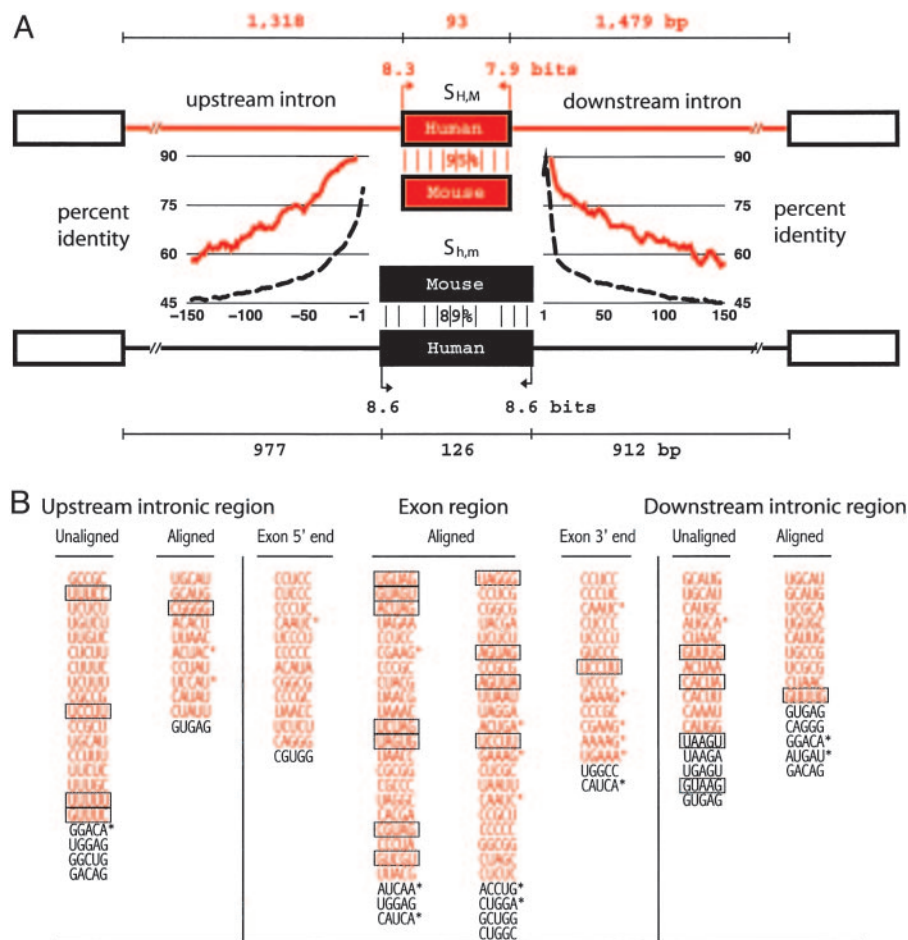


**Fig. 2.** Sequence features that differ between conserved alternative and constitutive human-mouse exons. (A) Features typical of exons of the  $S_{H,M}$  (alternatively spliced) and  $S_{h,m}$  (constitutive) training sets are depicted.  $S_{H,M}$  exons had shorter median exon length (93 versus 126 bases,  $P < 10^{-22}$ ), longer upstream intron length ( $P < 0.005$ ), longer downstream intron length ( $P < 10^{-5}$ ), weaker 5' and 3' splice site scores [ $P < 10^{-5}$  and  $P < 0.02$ , respectively; MAXENTSCAN (<http://genes.mit.edu>)], higher exon sequence conservation (percent identity;  $P < 10^{-46}$ ), and higher conservation (CLUSTAL W alignment score) in the 150-base intron regions immediately upstream and downstream of the exon ( $P < 10^{-63}$  and  $P < 10^{-66}$ , respectively). For each feature, the Kolmogorov-Smirnov test was used to test the null hypothesis of independent samples drawn from the same underlying population. Length and splice site score values are shown for human exons/introns; mouse values were similar. Average percent identity for alignments of flanking intron regions are shown in a 9-base sliding window for  $S_{H,M}$  (red trace) and  $S_{h,m}$  (black dashed trace) exons. (B) Pentanucleotides used by ACESCAN. Overrepresented (red) and underrepresented (black) pentamers in exon or 150-base flanking intron regions of  $S_{H,M}$  versus  $S_{h,m}$  exons. Pentamer frequencies were analyzed separately for CLUSTAL W-aligned regions only (aligned) or the entire region (unaligned). Exon 5' and 3' ends refer to the first and last 100 bases of exon, respectively. Boxed oligonucleotides indicate overlap with ESS hexamers (20), and oligonucleotides with asterisks indicate overlap with RESCUE-ESE hexamers (19).

We adapted a regularized least-squares classifier, which finds the optimal separating hyperplane in a high-dimensional space that distinguishes two classes of samples (21). Because it was not known *a priori* which of the 8,245 general and oligonucleotide features were most important in the classification scheme, models using different combinations of the eight general features and the region-specific oligonucleotide features were compared, and a feature selection protocol was used to reduce the number of parameters and to retain only the most relevant oligonucleotide features.

To determine the optimal features and parameters for the classifier, the training data were used to generate several models by varying (i) the choice of general features, (ii) the exon or intron regions from which oligonucleotide features were generated, and (iii) the number of most discriminative oligonucleotide features included. The model with the best performance used all of the general sequence features and 240 oligonucleotides with lengths of 4 and 5 bases (shown in Fig. 5, which is published as supporting information on the PNAS web site). This model assigned correct labels to  $\approx 90$  exon pairs for every 100 exon pairs drawn equally likely from  $S_{H,M}$  and  $S_{h,m}$ . For an individual exon, the ACESCAN score was defined as the mean of the classifier outputs over 50 random samplings of the training data. The distribution of ACESCAN scores for the exon pairs in  $S_{H,M}$  ranged from approximately  $-0.8$  to  $2.0$  (arbitrary units), compared to a range of approximately  $-1.8$  to  $0$  for most of the exons in  $S_{h,m}$  (Fig. 1). At a cutoff score of zero, only  $\approx 2\%$  of  $S_{h,m}$  exons had positive ACESCAN scores, compared with  $\approx 61\%$  of the exons in  $S_{H,M}$ , suggesting that ACESCAN[+] exon pairs are highly enriched for ACES.

**Experimental Validation of Conserved AS for 21 of 30 ACESCAN[+] Exon Pairs.** A combination of experimental tests and bioinformatic approaches was used to explore the features of ACESCAN[+] and

ACESCAN[-] exon pairs. First, the splicing patterns of a set of 30 arbitrarily chosen ACESCAN[+] exons were tested in a battery of human and mouse tissues by RT-PCR with primers targeted to flanking exons. ACESCAN[+] exons were selected from four intervals: I1 (ACESCAN score range, 0.0–0.5); I2 (ACESCAN score range, 0.5–1.0); I3 (ACESCAN score range, 1.0–1.5); and I4 (ACESCAN score,  $>1.5$ ), spanning the range of scores of most  $S_{H,M}$  exons. Panels of 12 normal human tissues and 8 normal mouse tissues were assayed. To avoid the undesired detection of aberrant or disease-specific splicing, tumor or other diseased tissues were not used. The products of these 600 RT-PCRs (30 exons  $\times$  20 tissues) were analyzed by gel electrophoresis, and the identities of PCR products with expected sizes for mRNAs including or excluding the test exon were confirmed by sequencing (Fig. 3A). In all, four of nine, seven of eight, six of eight, and four of five candidate ACES in intervals I1, I2, I3 and I4, respectively, were observed to undergo skipping in both human and mouse, whereas, for another two exons (both from interval I1), exon skipping was observed only in human tissues (Fig. 3; complete results are shown in Table 3, which is published as supporting information on the PNAS web site). Thus, of 30 predicted ACES interrogated by RT-PCR, 21 were observed to be skipped in human and mouse tissues, and high rates of validation of AS were seen in all four score intervals. These data support the presence of conserved AS in a majority of ACESCAN[+] exons. Although the 30 ACESCAN[+] candidates had no previous transcript evidence for skipping, searches of the literature and low-stringency searches of the cDNA and EST databases (August, 2004) identified possible evidence for a fraction of the AS events observed by RT-PCR, most often consisting of a single EST in only one species. In the examples studied, exon skipping was observed in many



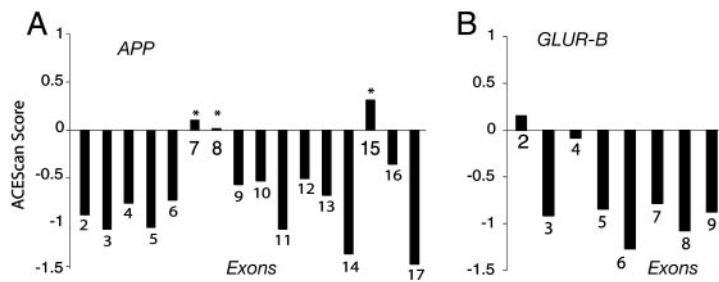


**Fig. 4.** ACESCAN scores for internal exons of well known alternatively spliced genes. Known alternative exons are indicated by asterisks; the known RNA edited exon of *GLUR-B* is indicated by the letter E. The following known AS exons are illustrated: exons 7 (168 bases), 8 (57 bases) and 15 (54 bases) of the human  $\beta$ -amyloid precursor protein precursor gene (*APP*, ENSEMBL Gene ID ENSG00000142192) (A) and exons 14 (115 bases) and 15 (249 bases) of the human glutamate receptor,  $\alpha$ -amino-3-hydroxy-5-methyl-4-isoxazolepropionic acid 2 gene (*GLUR-B*, ENSEMBL Gene ID ENSG00000120251) (B).

**Approximately 11% of EST-Derived AS Events Are Likely to Be Evolutionarily Conserved.** Of the  $\approx 4,300$  exon pairs with transcript evidence of skipping in human but not mouse (class  $S_{H,m}$ ), only  $\approx 7\%$  had positive ACESCAN scores (Fig. 1). Together with the observation that  $\approx 61\%$  of  $S_{H,M}$  exons were ACESCAN[+], this low fraction suggests that for only  $\approx 11\%$  (0.07/0.61) of the  $S_{H,m}$  exons is AS likely to be conserved in mouse. Thus, a surprising implication of these data is that the vast majority of the AS events inferable from human EST/cDNA-genomic alignments are not evolutionarily conserved in mouse. Instead, most of these events may represent aberrant, disease-specific, or allele-specific splicing (24) or events for which phylogenetic distribution is highly restricted.

**Functional Differences Between ACESCAN[+] and ACESCAN[-] Exons.** To assess potential functional differences between ACESCAN[+] and ACESCAN[-] exons that either have or do not have EST or cDNA evidence of exon skipping in human, we analyzed the density of SNPs and the frequency of reading frame preservation and protein domain disruption for each of these three classes of exon. Selective pressure on nucleotide sequence was assayed by mapping stringently filtered reference SNPs onto exons that had been scored by ACESCAN (Fig. 3B). This analysis found a  $\approx 50\%$  higher density of SNPs in ACESCAN[-]  $S_H$  exons than in ACESCAN[+] exons (this difference is significant at  $P < 10^{-5}$ ,  $\chi^2$  test), suggesting that ACES have been under much more stringent selection to conserve nucleotide sequence in recent human evolution than other exons. By contrast, ACESCAN[-]  $S_H$  exons appear to have experienced a degree of selection that was more similar to constitutive exons than to ACES.

Further evidence for the functional roles of many ACESCAN[+]  $S_H$  exons came from the observation that a far higher fraction of these exons had lengths that were multiples of three (68%, comparable with that seen in the training set of  $S_{H,M}$  exons) than was seen for ACESCAN[-]  $S_H$  exons, for which only  $\approx 43\%$  had lengths divisible by three, near background levels for constitutive internal exons (Fig. 3C). This difference is highly significant ( $P < 10^{-15}$ ,  $\chi^2$  test) and implies the existence of strong selection on the alternative protein products derived from alternative splicing of ACESCAN[+] exons. Notably, divisibility of the exon length by three was not used in the predictions (only the general size of the exon, with shorter lengths favored over longer lengths).

The frequency of disruption or removal of a protein domain by AS has been studied by several groups (e.g., refs. 25–27). We found that only  $\approx 37\%$  of ACESCAN[+] exons overlapped ORF regions encoding INTERPRO-annotated protein domains by 30 bases (10 codons) or more, a significantly lower fraction than for ACESCAN[-] exons studied of either the  $S_H$  or  $S_I$  classes (Fig. 3D), both of which had similar frequencies of domain disruption ( $\approx 50\%$ ). Reducing the minimum overlap to 15 bases gave similar results (data not shown). This finding is generally consistent with the results of Kriventseva *et al.* (26), who observed that protein isoforms arising from AS are more likely to preserve protein domain structure than is expected by chance. Taken together, the data shown in Fig. 3 consistently demonstrate that ACESCAN[+] exons are under strong selection to conserve function, both at the nucleotide level (Fig. 3B)

and at the level of the encoded alternative protein isoform (Figs. 3C and D). In contrast, ACESCAN[-] exons show less evidence of selective constraints at the nucleotide level (Fig. 3B), and there is little if any evidence of additional constraints on the protein products derived from exon skipping of ACESCAN[-] exons, even when there is transcript evidence that such skipping occurs (Figs. 3C and D).

**Applications of ACESCAN at the Gene Level.** Application of ACESCAN to well studied genes illustrates some of the strengths and limitations of our approach (*APP* and *GLUR-B* shown in Fig. 4; *PTB* and *CACNA1G* shown in Fig. 6, which is published as supporting information on the PNAS web site). Of the identifiable orthologous human/mouse exon pairs in these genes, known exon skipping events (asterisks in Fig. 4) all received positive ACESCAN scores, implying that their skipping is likely to be conserved in mouse. Skipping of exons 7 and 8 of the  $\beta$ -amyloid precursor protein gene (*APP*) implicated in Alzheimer's disease was detected successfully in a recent large-scale microarray analysis of AS in human tissues (28). These exons, as well as exon 15 of the *APP* gene, received positive ACESCAN scores (Fig. 4A); all three of these exons are known to undergo exon skipping (29, 30). The *GLUR-B* gene, one of the four *GluR* subunits that assemble to form the  $\alpha$ -amino-3-hydroxy-5-methyl-4-isoxazolepropionic acid glutamate receptor, contains two well known skipped exons (flip and flop, exons 14 and 15, respectively), both of which received positive ACESCAN scores, as well as an exon (exon 13, which is marked with an E in Fig. 4) that undergoes RNA editing (31). This edited exon and the downstream intron form an RNA hairpin and are highly conserved in sequence (31). Despite this high level of exonic and intronic sequence conservation, this exon received a negative ACESCAN score (Fig. 4B), providing an example of the specificity of our method for AS exons. A web server has been set up (<http://genes.mit.edu/acescan>) that provides access to the training sets of all ACESCAN plots for ENSEMBL-annotated orthologous human/mouse gene pairs.

Recently, Bejerano *et al.* (32) reported 111 exonic ultraconserved regions of  $\geq 200$  bases with 100% sequence identity between the human and mouse genomes, most of unknown function. Comparing these with our predicted ACES, 33 of the 37 ultraconserved regions ( $\approx 89\%$ ) that mapped to internal exons that could be scored by ACESCAN received positive ACESCAN scores, suggesting that a number of these elements correspond to ACES.

**Functional Characteristics of ACESCAN[+] Genes.** In total, 1,550 genes were identified, containing 2,092 ACESCAN[+] exons,  $\approx 85\%$  of which lacked prior transcript (EST/cDNA) evidence for exon skipping. Initial comparisons to the partially annotated rat genome showed a high correlation between human–mouse and human–rat ACESCAN scores, as expected (data not shown). To determine whether genes that contain ACESCAN[+] exons, which we refer to as ACESCAN[+] genes, are biased toward particular biological activities, we compared these genes to the set of genes not found to contain any ACESCAN[+] exons (ACESCAN[-] genes) by using Gene Ontology (GO) classifications ([www.geneontology.org](http://www.geneontology.org)), as in refs.

